Activation of mGluR1 Mediates C1q-Dependent Microglial Phagocytosis of Glutamatergic Synapses in Alzheimer's Rodent Models

Presenting Author: Jiang Wu[1]

Co-Authors: Bihua Bie[1], Joseph F. Foss[1], Mohamed Naguib[1]

[1]Department of General Anesthesia, Anesthesiology Institute, Cleveland Clinic

Introduction: Brains of patients with Alzheimer's disease (AD) are characterized by neuroinflammation and synaptic loss. Microglia and complement appear to be involved in the synaptic and cognitive deficits seen in AD, though the mechanisms remain elusive. Our hypothesis is illustrated in **Fig. 1**.

Methods: Two types of rodent models of Alzheimer's disease, rats injected with amyloid fibrils into hippocampal CA1 and transgenic APP/PS1 mice, were used in this study. Immunostaining was applied to study the microglia phagocytosis of glutamatergic synapse, which was analyzed by confocal 3-D image. Immunoblotting was used to study the expression of C1q and other proteins. Whole-cell recording and Morris water maze were used to evaluate the synaptic and cognitive function in the rodent models.

Result: First, we noted an increased complement C1q-mediated microglial phagocytosis of the hippocampal glutamatergic synapses that resulted in synaptic and cognitive deficits in both models of AD (**Fig. 2**). We also found an increased activity of the metabotropic glutamate receptor 1 (mGluR1) in the hippocampal CA1 area. Suppression of mGluR1- protein phosphatase 2 (PP2A) signaling inhibited the dephosphorylation of FMRP and repressed the local translation of synaptic C1q mRNA (**Fig. 3**), which consequently alleviated the microglial phagocytosis of synapses in the hippocampal CA1 and restored the synaptic and cognitive function in the rodent models (**Fig. 4**). Artificial activation of mGluR1 signaling by DHPG promoted dephosphorylation of fragile X mental retardation protein (FMRP) and facilitated the local translation machinery of synaptic C1q mRNA (**Fig. 5**) —mimicking the C1q-mediated microglial phagocytosis of hippocampal glutamatergic synapses and synaptic and cognitive deficiency in the rat model (**Fig. 6**).

Conclusion: Our findings demonstrated that activation of mGluR1-PP2A signaling by amyloid fibrils induced the dephosphorylation of FMRP, which facilitated the local translation of C1q mRNA in both rodent models. This led to C1q-mediated microglial phagocytosis of hippocampal glutamatergic synapses, which contributed to the development of synaptic and cognitive deficiency in AD.

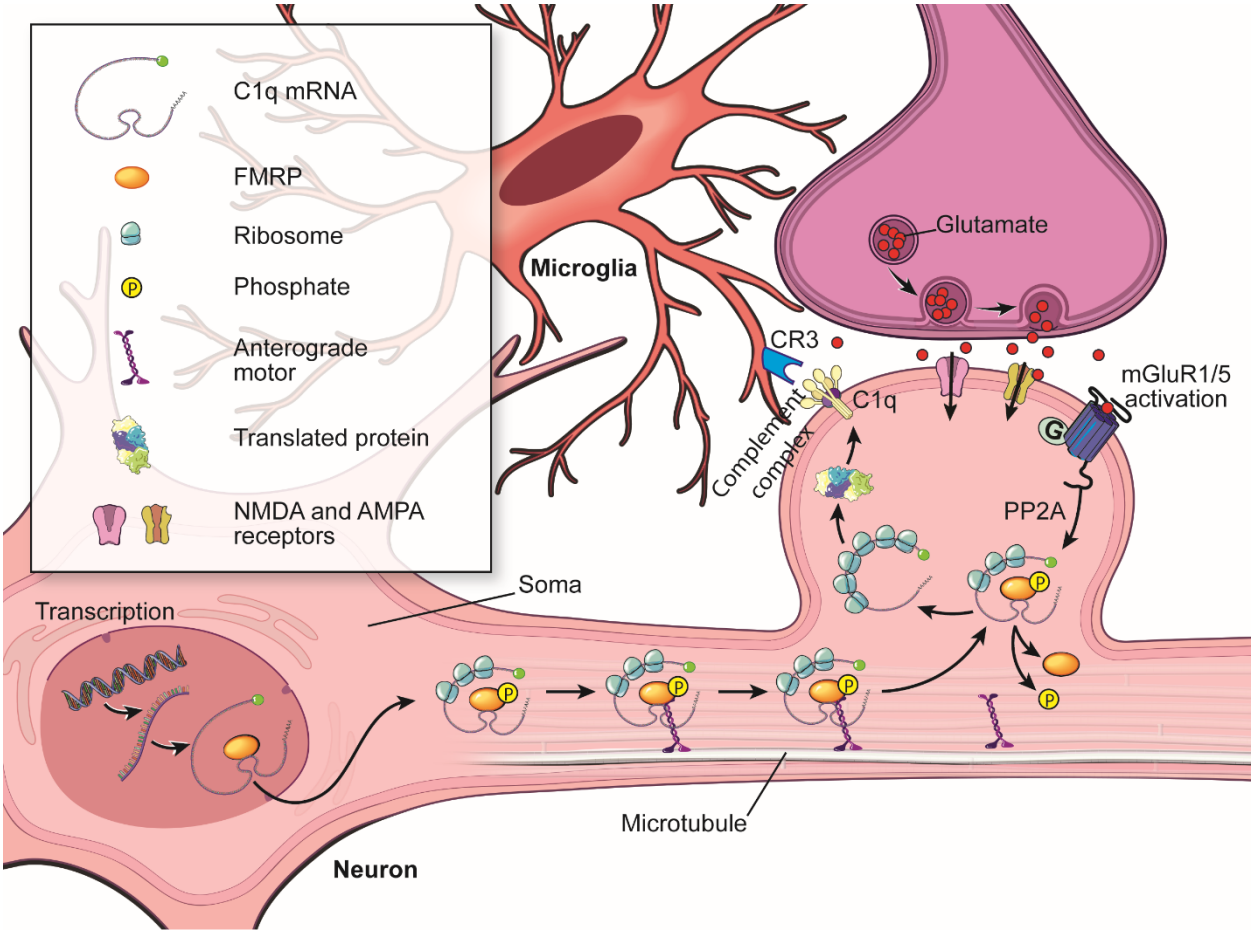

Figure 1. Hypothesis tested. Abnormal accumulation of amyloid fibrils induces substantial neuroinflammation (e.g., microglial activation) and the upregulation of mGluR1 signaling in the hippocampal CA1. Activation of mGluR1 signaling induces remarkable PP2A activity, which triggers the dephosphorylation of FMRP in the glutamatergic synapses. This adaptation of translational machinery, in turn, facilitates the transport and local translation of synaptic C1q mRNA in the glutamatergic synapses. The increased expression of C1q in glutamatergic synapses initiates the complement response leading to CR3 opsonization in the activated microglia, which eventually triggers the microglial phagocytosis of hippocampal glutamatergic synapses, thus contributing to the synaptic dysfunction and memory deficiency induced by amyloid fibrils.

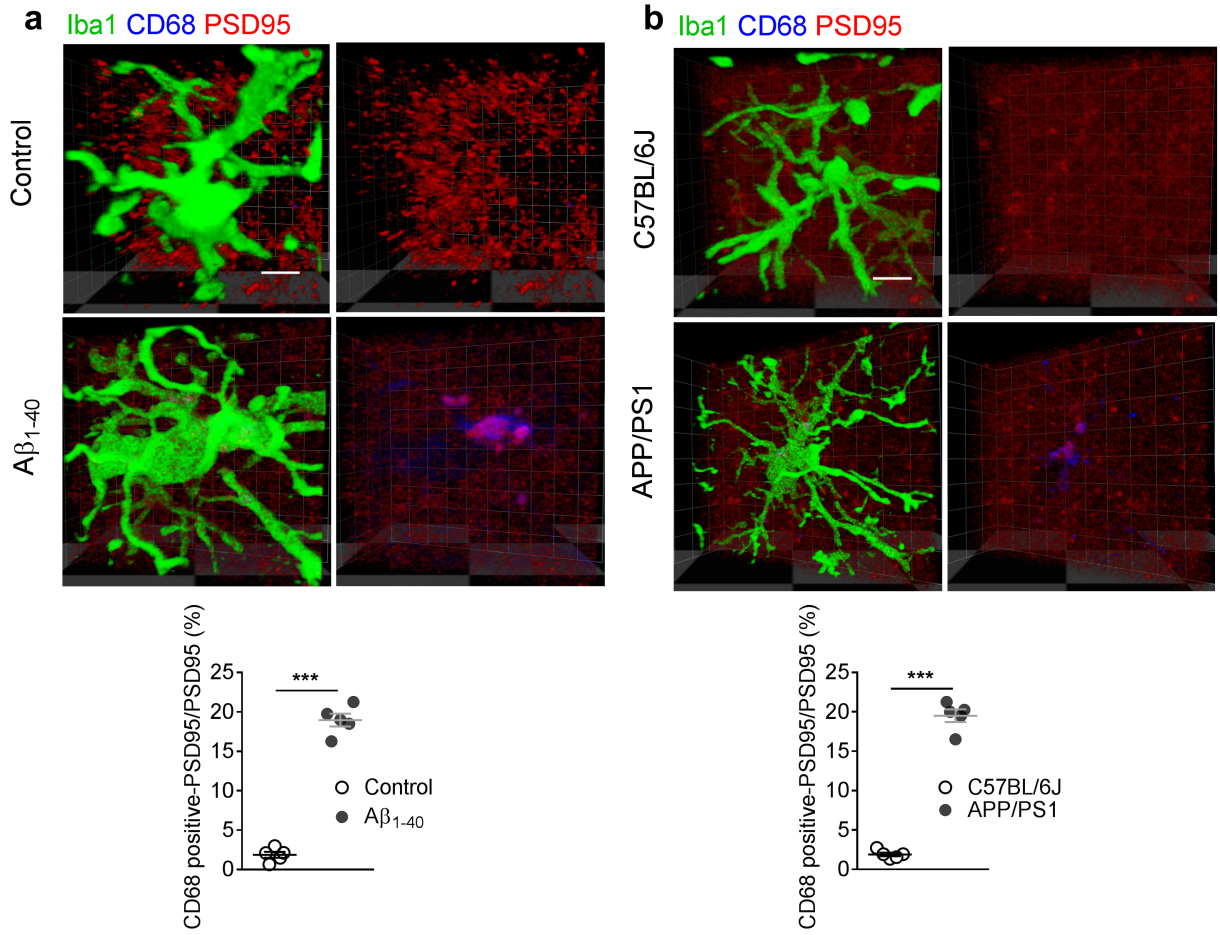

Figure 2. Increased microglial phagocytosis of glutamatergic synapses in rodent AD model. Increased internalization of postsynaptic marker PSD95 was observed in the lysosomes (CD68) within the microglia (Iba1) in the rats injected with $A\beta_{1–40}$ fibrils (***a***, n = 5 rats in each group, t = 18.9, DF = 8, two-tailed P <0.0001, scale bar = 10 μm). A micrograph was presented at the right to show the same microglia in which only the lysosomes (blue) and PSD95 (red) were visualized. Similar increases in co-localization of PSD95 with lysosome marker CD68 within the microglia were observed in the hippocampal CA1 of the Tg-APPsw/PSEN1DE9 (APP/PSI) mice (***b***, n = 5 mice in each group, t = 21.6, DF = 8, two-tailed P <0.0001, scale bar = 10 μm). Data represent mean ± s.e.m. ***P<0.001. Each dot represents the mean value of 4 brain slices of one animal.

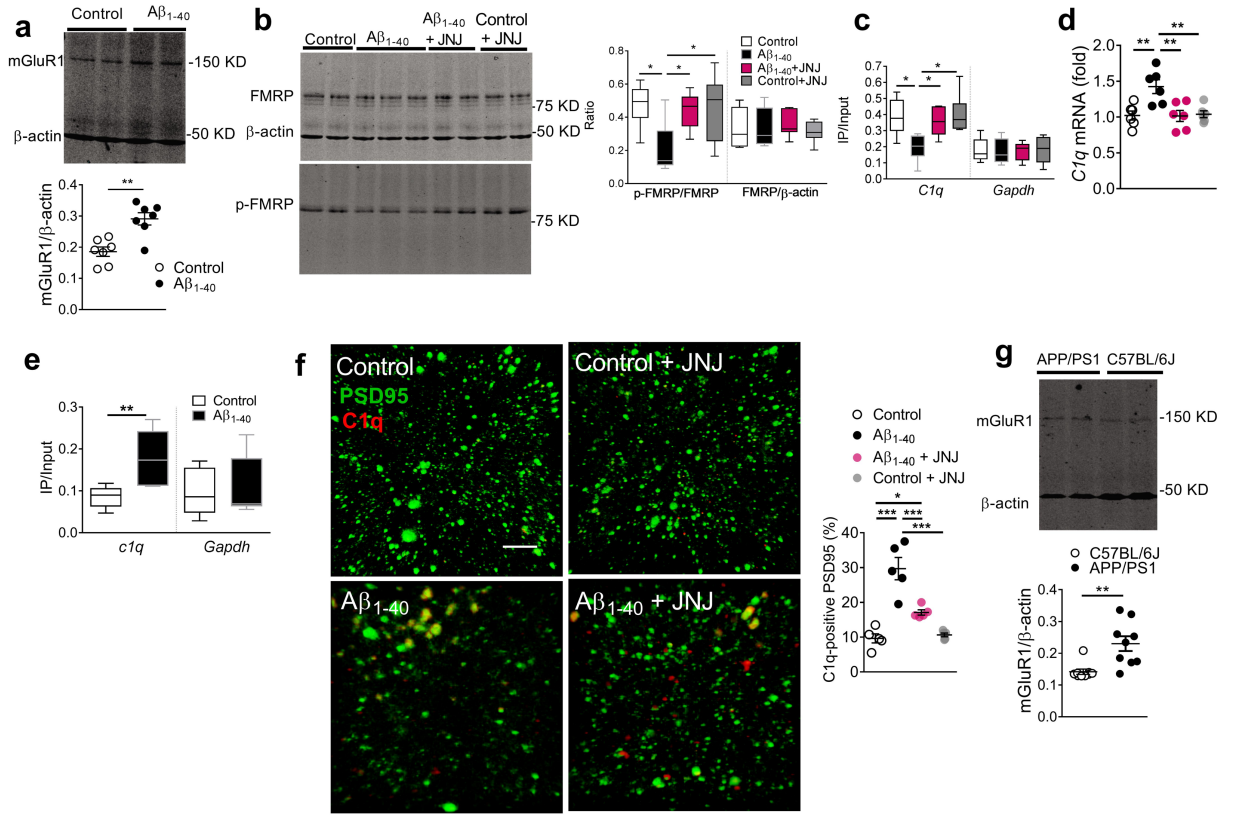

Figure 3. Inhibition of metabotropic glutamate receptor 1 (mGluR1) signaling attenuated the C1q upregulation induced by amyloid fibrils. Significantly increased expression of mGluR1 was observed in the hippocampal CA1 in the rats injected with amyloid fibrils (**a**, n = 7 rats in each group, t = 4.3, DF = 12, two-tailed P = 0.001). Amyloid fibrils decreased the phosphorylation of fragile X mental retardation protein (FMRP) in the hippocampal CA1, which was recovered by the mGluR1 inhibitor JNJ16259685 (**b**, n = 6,7,7,7 rats, $F_{3,23}$ = 4.3, P = 0.015); (**c**) RNA-IP study revealed a significantly decreased amount of C1q mRNA pulled-down by p-FMRP antibody in the hippocampal CA1 in the modeled rats, which was recovered by JNJ16259685 (**c**, n = 6 rats in each group, $F_{3,20}$ = 4.97, P = 0.009). Significantly increased *C1q* mRNA was detected in the hippocampal synaptosomal preparation in the modeled rats, which was attenuated by JNJ16259685 (**d**, n = 6 rats in each group, $F_{3,20}$ = 7.46, P = 0.002). Increased C1q mRNA was pulled by e-IF4E antibody in hippocampal CA1 lysates of the rats injected with amyloid fibrils (**e**, n = 6 rats per group, t = 3.3, DF = 10, two-tailed P = 0.009). For box-and-whiskers plots, the box extends from the 25th to 75th percentiles, a line within the box marks the median. Whiskers (error bars) above and below the box represent the minimum and maximum values. Microinjection of JNJ16259685 significantly decreased C1q immunosignals co-localized with the PSD95 in the hippocampal CA1 in the amyloid-injected rats (**f**, n = 5 rats in each group, $F_{3,16}$ = 26.5, P <0.0001, scale bar = 10 μm). Each dot represents the mean value of 4 brain slices of one rat. Significantly increased expression of mGluR1 was observed in the hippocampal CA1 in the Tg-APPsw/PSEN1DE9 (APP/PSI) mice (**g**, n = 9 mice in each group, t = 3.6,

DF = 16, two-tailed P = 0.003). Data represent mean ± s.e.m. *P<0.05, **P<0.01, ***P<0.001.

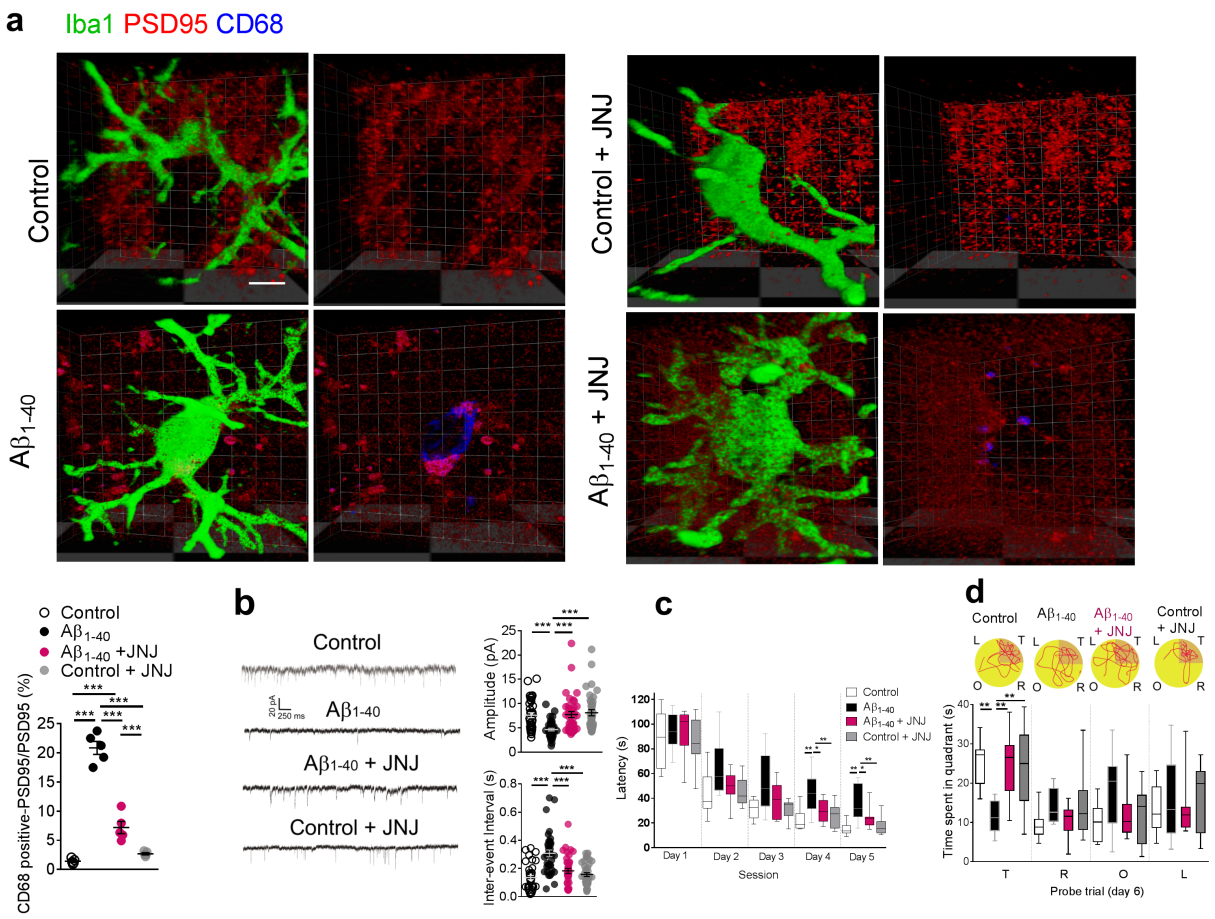

Figure 4. Inhibition of mGluR1 signaling attenuated the microglia phagocytosis of synapses induced by amyloid fibrils. JNJ16259685 significantly decreased the co-localization of PSD95 with lysosome marker CD68 in microglia (Iba1) in the rats injected with amyloid fibrils (**a**, n = 5 rats in each group, $F_{3,16}$ = 301.8, P <0.0001, scale bar = 10 μm). Right micrographs were presented to show the same microglia in which only the lysosomes (blue) and PSD95 (red) were visualized. Microinjection of JNJ16259685 significantly recovered the amplitude (**b**, n = 38 neurons in each group, Kruskal-Wallis Statistic KW = 33.6, P<0.0001) and inter-event interval of mEPSCs (**b**, n = 38 neurons in each group, Kruskal-Wallis Statistic KW = 37.9, P<0.0001) in the hippocampal CA1 neurons in the rats injected with amyloid fibrils. Microinjection of JNJ16259685 also shortened the escape latency (**c,** n = 10 rats in each group, effect of group [$F_{3,36}$ = 13.3, P<0.0001], effect of time [$F_{4,36}$ = 135.5, P<0.0001], interaction between group and time [P = 0.47]) and increased the time spent in the target quadrant (**d,** n = 10 rats in each group, $F_{4,36}$ = 6.57, P = 0.0012) in the amyloid-injected rats. (**d**) Representative path tracings in each quadrant during the probe trial on day 6 (T, target quadrant; R, right quadrant; O, opposite quadrant; L, left quadrant). Data represent mean ± s.e.m. For box-and-whiskers plots, the box extends from the 25th to 75th percentiles, a line within the box marks the median. Whiskers (error bars) above and below the box represent the minimum and maximum values. *P<0.05, **P<0.01, ***P<0.001.

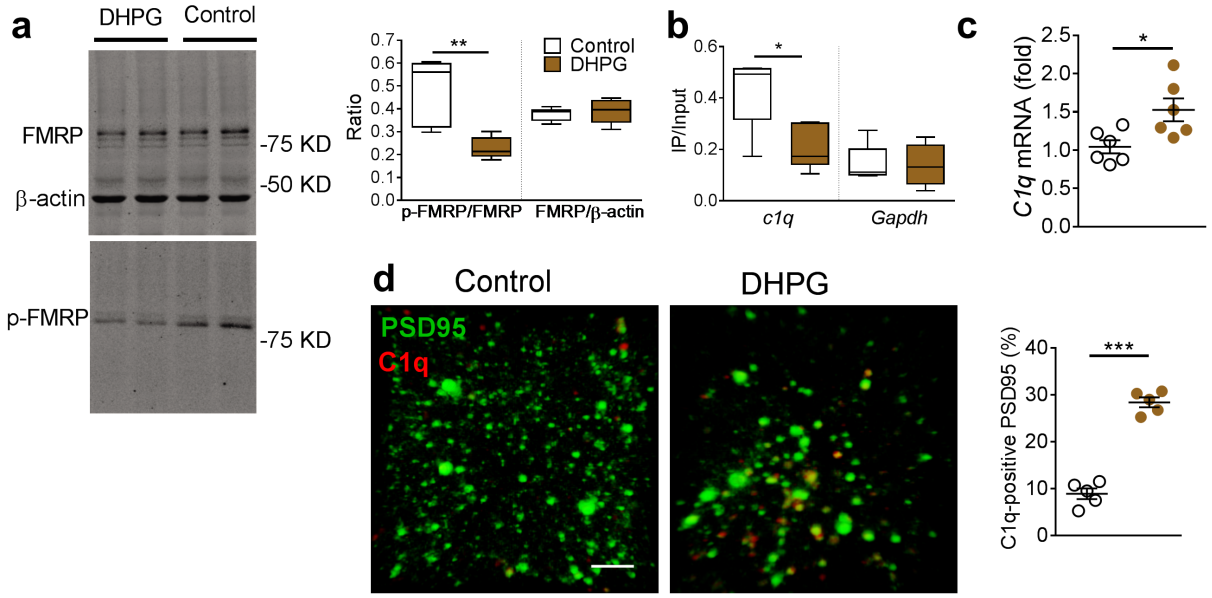

Figure 5. Activation of mGluR1 signaling by specific mGluR agonist dihydroxyphenylglycine (DHPG) upregulated hippocampal C1q expression. Microinjection of DHPG into the hippocampal CA1 in naïve rats induced dephosphorylation of FMRP (**a**, n = 6 rats in each group, Mann-Whitney U-statistic = 35.00, two-tailed P = 0.007), decreased the binding between phosphorylated FMRP (p-FMRP) and *C1q* mRNA (**b**, n = 6 rats in each group, Mann-Whitney U-statistic = 33.00, two-tailed P = 0.015), and increased *C1q* mRNA in the hippocampal CA1 synaptosome (**c**, n = 6 rats in each group, t = 2.8, DF = 10, two-tailed P = 0.018). DHPG also increased the C1q immunosignal co-localized with PSD95 in the hippocampal CA1 in the naïve rats (**d**, n = 5 rats in each group, t = 12.6, DF = 8, two-tailed P <0.0001, scale bar = 10 μm). Each dot represents the mean value of 4 brain slices of one rat. Data represent mean ± s.e.m. For box-and-whiskers plots, the box extends from the 25th to 75th percentiles, a line within the box marks the median. Whiskers (error bars) above and below the box represent the minimum and maximum values *P<0.05, **P<0.01, ***P<0.001.

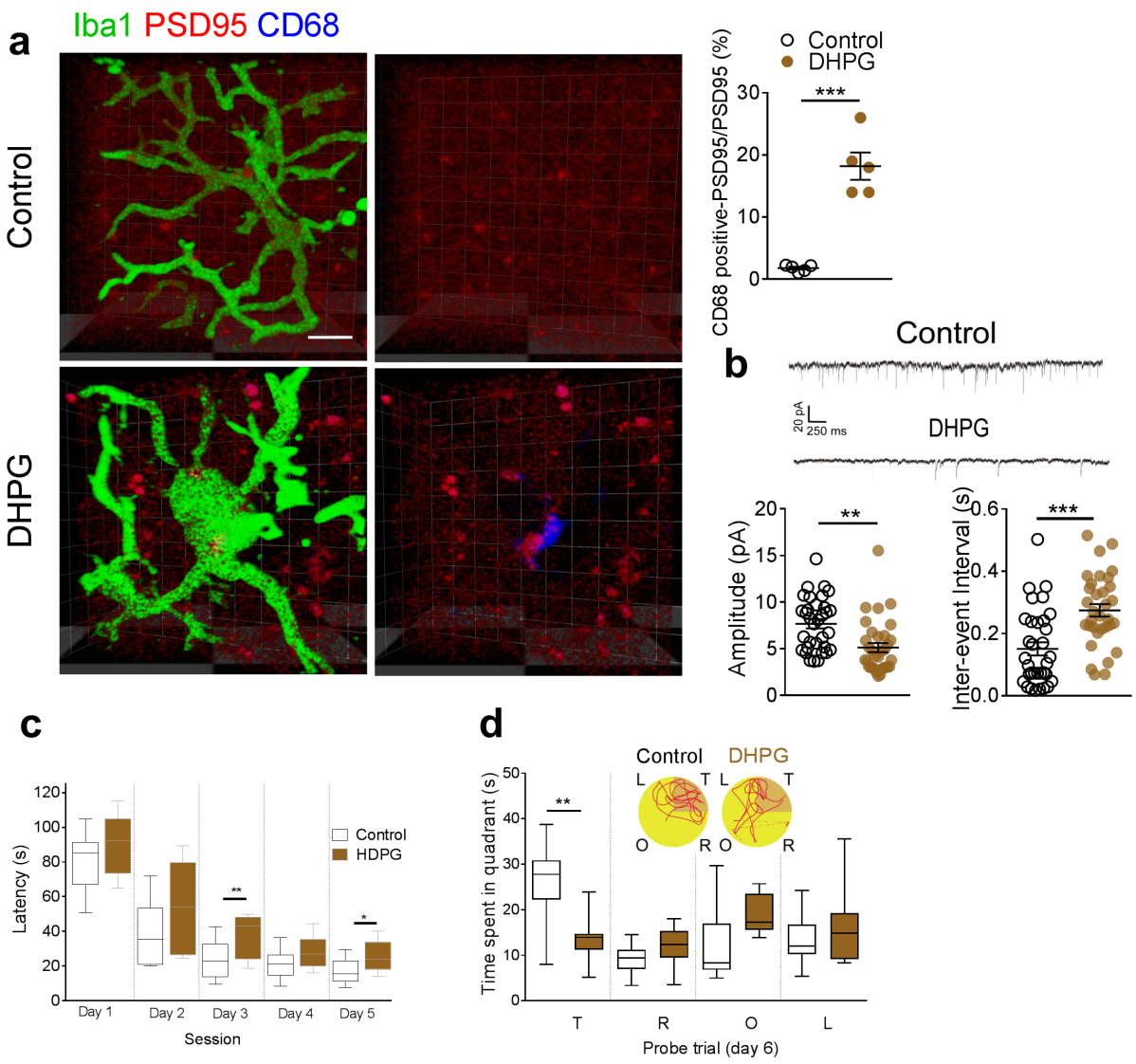

Figure 6. Activation of mGluR1 signaling by DHPG induced the microglial phagocytosis of glutamatergic synapses. DHPG increased the co-localization of PSD95 with the lysosome marker CD68 in microglia in the hippocampal CA1of naïve rats (**a**, n = 5 rats in each group, t = 7.4, DF = 8, two-tailed P <0.0001, scale bar = 10 μm). Right micrographs were presented to show the same microglia in which only the lysosomes (blue) and PSD95 (red) were visualized. Each dot represents the mean value of 4 brain slices of one rat. DHPG also decreased the amplitude (**b**, n = 33 neurons in each group, t = 3.7, DF = 64, two-tailed P = 0.0005) and increased inter-event interval (**b**, n = 33 neurons in each group, t = 4.2, DF = 64, two-tailed P <0.0001) of mEPSCs in hippocampal CA1 neurons, and increased escape latency (**c,** n = 10 rats in each group, effect of group [$F_{1,18}$ = 8.2, P = 0.01], effect of time [$F_{4,18}$ = 82.8, P<0.0001], interaction between group and time [P = 0.52]), and decreased the time in the target quadrant (**d**, n = 10 rats in each group, $F_{1,18}$ = 14.4, P = 0.001). (**d**) Representative path tracings in each quadrant during the probe trial on day 6 (T, target

quadrant; R, right quadrant; O, opposite quadrant; L, left quadrant). Data represent mean ± s.e.m. For box-and-whiskers plots, the box extends from the 25th to 75th percentiles, a line within the box marks the median. Whiskers (error bars) above and below the box represent the minimum and maximum values. *P<0.05, **P<0.01, ***P<0.001.